DOI: 10.55522/jmpas.V11I2.2159 ISSN NO. 2320–7418

International peer reviewed open access journal

Journal of Medical Pharmaceutical and Allied Sciences

Journal homepage: www.jmpas.com CODEN: JMPACO

Research article

Nano-sized Liposomes for nose to brain delivery of Carmustine Formulation, Optimization by Box Behnken design

M Alagusundaram[1], K B ChandraSekhar[2], G Nethra Vani[3]*

[1] [2]Department of Pharmaceutics, Ratnam Institute of Pharmacy, Nellore, Andhra Pradesh
[3]Department of Chemistry, Jawaharlal Nehru Technological University, Anantapur, Andhra Pradesh
[3]Department of Pharmaceutical Sciences, Jawaharlal Nehru Technological University, Anantapur, Andhra Pradesh

ABSTRACT

Successful treatment of glioma remains a hard challenge. This study aims at the development and assessment of nano sized liposomal vesicles (NSL) loaded with Carmustine (CS) for the treatment of glioma. The experimental NSLs were developed by conventional lipid layer hydration technique and were characterized by different parameters such as % Entrapment efficiency, zeta potential, scanning electron microscopy (SEM), transmission electron microscopy (TEM), *in vitro* drug release study. The optimized Carmustine nanosized liposomes (OCS-NSLs) presented the practical values of % EE of CS is 94.27 ± 0.25%, particle size of 235.65 ± 12.87 nm and *in vitro* drug release of CS 97.089 ± 1.76%. On the base of the polynomial equation, it was resolved that as the total lipid to drug concentration increases, the % EE of optimized formulation and this leads to more space for the accommodation of drug particle, likewise addition of lipid content as well reduces the escaping of drug into the external phase. OCS-NSLs were spherical in shape with a smooth surface as depicted from SEM data. A TEM study confirmed formation of vesicles with intact outer bilayer. *In vitro* drug release of 95.67± 1.54% was reported for the OCS-NSLs along with a sustained release of CS over a 24 h study period with desired kinetic values. Hence, the optimized formulation has shown a better response on Carmustine loaded nano liposomal formulation for intranasal application.

Keywords: Carmustine, Glioma, Nanosized lipid vesicles. New drug delivery, CNS.

Received - 13-10-2021, Accepted- 24-02-2022

Correspondence: G Nethra Vani* ✉ nethravani.g@gmail.com

Department of Pharmaceutical Sciences, Jawaharlal Nehru Technological University, Anantapur, Andhra Pradesh, India

INTRODUCTION

Glioma is the primary cerebral tumour. It is the most destructive type of tumour among humans. Patients with glioblastoma (GB) have a survival rate of 8 to 14 months after diagnosis [1]. Surgery, chemo and radiation therapy are available in GB. A challenge in the treatment of glioma is the blood-brain barrier (BBB), which consists of tight specialist and endothelial junctions lining the central nervous system. It is proposed that many drug molecules are effective in treating brain tumours but failin clinical trials. This is due to the inability to enter the blood-brain barrier (BB). Therefore, there is a need for improved drug administration strategies [2-4].

In certain cases, oral route fails to deliver the therapeutic amount of drug to brain due to the presence of certain interfaces like blood–brain barrier (BBB), blood–cerebrospinal fluid barrier (BCSFB) and efflux transporters (AET) [5]. These barriers control the exchange between the peripheral blood flow and the cerebrospinal fluid circulatory system (CSF). Other factors, such as the physicochemical properties of the drug, also interfere with central nervous system (CNS) administration [6]. Therefore, several approaches like BBB disruption, drug manipulation and alternative route of drug administration like intra cerebral ventricular, intrathecal and olfactory pathways (intranasal route) are being used for targeting of drugs to the brain [7]. In the present scenario, the intranasal route to bypass the BBB is an upcoming field, as this route caters a novel, practical, simple and non-invasive approach to bypass the BBB and reduce the systemic exposure and thus systemic side-effects associated with drug [8]. Drug after intranasal administration reaches the olfactory epithelium region of the nasal mucosa that acts as a gateway for substances entering the CNS due to the neural connection between the nasal mucosa and the brain [9].

Carmustine (CS) has recently been used as a drug to treat glioma [10-12]. However, it has been restricted as a result of side effects such as bone marrow suppression [13] and pulmonary fibrosis [14]. To reduce toxicity, gliadel wafers [15] were impregnated with CS. These gliadel wafers were not successful as they do not show effective therapeutic efficacy due to poor penetration, inability to prevent tumor recurrence, lack of synergistic action with other

chemotherapeutic drugs and/or radiotherapy [16]. To overcome these problems, a variety of drug distribution vehicles have recently been developed. These include liposomes, nanoshells, dendrimers, polymeric micelles, carbon nanotubes, polyglycolicacid (PGA) nanoparticles, polylactic acid (PLA) nanoparticles, and poly (D, L-lactic-coglycolides) acid (PLGA) nanoparticles [17, 18].

This study hypothesizes that CS nano-sized liposomes was designed to formulate a design optimized nano lipid mediated intranasal delivery of Carmustine for better targeting and effective therapeutic outcome.

MATERIALS AND METHODS

Carmustine (CS) was obtained as a gift sample from SP Accure Labs Private Ltd., Telangana, India. Cholesterol (CHL), Soya-L-α-lecithin (SL), was procured from Merck (Mumbai, India). Chloroform was purchased from Hi Media Laboratories Pvt. Ltd (Mumbai, India). U87MG human glioma cells were procured from National Center for Cell Science (Pune, India). All other chemicals used in the experiment were of analytical grade.

Compatibility study of selected excipients with drug

The compatibility between lipid, cholesterol and the drug has been identified using Fourier transform infrared spectrophotometer (Bruker FTIR alpha spectrophotometer, Billerica, MA). IR spectra of drug, lipid, cholesterol and physical mixture of drug, lipid and cholesterol were scanned from 4000 cm^{-1} to 400 cm^{-1} and recorded [19].

Formulation of Nano sized Liposomes

Nanosized liposomes (NSL) loaded with investigational drug were prepared using a conventional thin-film hydration method with the required change in process parameters [20]. For preparing NSL loaded with CS (CS-NSLs), SL was used as the primary phospholipid. Briefly, weighed amount of CS, SL and CHL were dissolved in a required volume of chloroform taken in a 250 ml round bottom flask. The prepared mixture was then subjected to gentle rotation along with the evaporation of the solvent in a rotary vacuum evaporator (R-150, Super fit Continental Private Limited, Mumbai, India), connected with a water bath. The temperature of the water bath was kept at 40 °C. Following evaporation of the chloroform, a thin film formed along the inside wall of the round-bottomed flask. The flask was then stored in a desiccator overnight, which resulted in the removal of any residue of organic solvent still present in the thin film. The formed thin film was hydrated with phosphate buffer saline (PBS), pH 7.4 for 1 h. After hydration, the blend was subjected to sonication in a so nicator (Q Sonica, Cole-Parmer India Pvt. Ltd. Mumbai, India). Sonication makes it possible to reduce the large vesicles in the desired ultra-small size range. After sonication, the formulation was allowed to rest for 1 hour at room temperature, and then kept in the refrigerator overnight at 4°C. Lastly, the sample was dried in a lyophilizer using propylene glycol (Esquire Biotech, Chennai, India) to obtain a dried mass of the sample.

BBD Design for Optimization of Nano sized Liposomes

A three factors three levels Box–Behnken experimental design was used for optimization and to evaluate the relationship between the independent variables like drug to lipid ratio(X1), Cholesterol (X2) and Sonication time (X3) and dependent (responses) variables, i.e., Entrapment efficiency (Y1), Particle size (Y2) and *in vitro* drug release (Y3). Consequently, by setting the independent variables, we studied at three different levels: low (-1), medium (0) and high (+1) (Table 1). Different batches (F1–F17) were prepared and data were substituted in design expert. The design included 17 tests (as shown in Table 2) with the computer-generated quadratic equation as follows:

$$Y = b0 + b_1X_1 + b_2X_2 + b_3X_3 + b_{12}X_1X_2 + b_{13}X_1X_3 + b_{23}X_2X_3 + b_{11}X_1^2 + b_{22}X_2^2 + b_{33}X_3^2$$

Where Y is the measured response for each factor level combination,b_0 is constant, b_1, b_2, b_3 are linear coefficients, whereas b_{12}, b_{13},b_{23} are the interaction coefficients in the mid of the 3 factors, henceb_{11}, b_{22}, b_{33} are the quadratic coefficients of the observed experimental values, and X1, X2 and X3 are values for the independent variables. Furthermore, the optimal formulation was selected using the point-based numerical prediction method using the desirability function. Finally, linear regression with ANOVA was utilized to choose the most suitable model and p values below 0.05 were considered statistically significant.

Table 1: Independent and dependent variables used in Box–Behnken design for the development and optimization

Factor	Level used, actual coded		
Independent variables	Low (-1)	Medium (-1)	High (+1)
X1=Drug to lipid ratio	1:3	1:4	1:5
X2=Cholesterol (mg)	5	15	25
X3=Sonication time (min)	5	10	15
Dependent variables	Goal		
% EE(Y1)	Maximize		
Particle size (nm) (Y2)	Maximize		
In vitro release (%) (Y3)	Maximize		

Characterization of Prepared NSL

Particle size, PDI and Surface Charge

The particle size and Polydispersity Index (PDI) of the optimized formulations were determined by Zetasizer 1000HS (Malvern Instruments, UK) using photon correlation spectroscopy. Before testing, the samples were diluted with Phosphate buffered saline (PBS) and filtered using a 0.45 µm membrane filter [21]. Zetasizer (Malvern Instruments, Malvern, UK) was used to identify the surface charge of the trapped vesicle. The average zeta potential of the vesicles was determined [22, 23]. These values are based on three distinct experiments, each with three replications.

% Entrapment efficiency

The ultracentrifugation technique was applied to learn the percent entrapment efficiency (% EE) of CS in all formulations using

Ultracentrifuge (Remi lab, Mumbai, India) equipped with SW60 Ti Rotor at 60,000 revolutions per minute at 4 °C for 1.5 h. Free CS was determined from a supernatant solution after centrifuging and dilution with milliQ water. The total amount of CS in the formulation was measured after rupturing the vesicles with methanol to a ratio of 1:1 in the sample and methanol. All samples were filtered through a 0.45 µm syringe filter membrane and the PR content was tested using a UV spectrophotometer. All determinations were made in triplicate and the % EE was computed [24].

$$\% EE = \frac{T - F}{T} \times 100$$

Where, % EE is the percent entrapment efficiency, T is the total amount of CS in the formulation and F is the free CS amount.

Vesicular shape and surface morphology

Vesicular shapeand surface morphology were analyzed using, transmitting electron microscopy (TEM) (Jeol electron microscope, Japan). The NSL was diluted in an appropriate solvent, and a drop of the solution was placed on the carbon-covered grid with a sheet of paraffin wax, stored for 1 min. Then the grid was dried at room temperature and placed along the drop of phosphotungstate for 10 s, and the sample was examined by TEM [25].

Scanning Electron Microscopy

Morphology of prepared NSL-OCS have been determined using scanning electron microscopy (SEM) JSM 5610 LV SEM, JEOL, Japan). The nano-size lipid carrier was diluted in a suitable solvent, and a drop of NSL was mounted on gold coated metal stubs, under vacuum and then analyzed using SEM [26].

***In vitro* drug release study**

For the *in vitro* drug release study of the OCS-NSLs, the conventional dialysis method was employed [27, 28]. For the experiment, a weighed amount of OCS-NSLs was dispersed in PBS containing 0.5% w/v sodium lauryl sulfate (SLS) as a solubilizing agent (release medium) and an equivalent amount of free-drug suspension were reconstituted with 1mL drug release media and poured into a dialysis bag. Both ends of the dialysis bag were attached with the wire and the entire system was submerged in a beaker containing 100 ml of the above release medium. Subsequently, the beaker was placed on a magnetic stirrer at a rotation of 300 revolutions per minute by means of a magnetic bead. At different time intervals for 24 hours, 1 ml of sample was taken from the beaker with simultaneous replacement of the fresh release medium to maintain the state of the sink. The experiment was carried out for 24 h. The samples after collection were filtered with the help of membrane filter followed by measurement of the absorbance at 227 nm in PBS containing SLS was taken as the blank during measurement [29].

Estimation of drug release kinetics

Release kinetics helps to predict the mechanism of drug release from the tested OCS-NSLs. To achieve this, data from *in vitro* drug release studies were integrated into various kinetic models. We found out the release form in three different models such as null-order (cumulative total of drug released Vs time), Higuchi (cumulative total of drug released Vs square root of time), Korsmeyer–Peppas (logarithmic value of the accumulated total of drug released Vs logarithmic value of time) [30-32]. The linearity of the graphs was evaluated based on the computed R^2 values.

RESULTS AND DISCUSSION

Compatibility study of selected excipients with drug

The compatibility between the drug, lipids and cholesterol was determined by FTIR spectrophotometer. FTIR spectrum of CS showed the characteristic peaks of the drug structure shown in Figure 1. The pure drug (CS) exhibited the peaks at 1256 and 1448 cm^{-1} belong to COO^- groups,1135 cm^{-1} corresponds to C=H double bond. Also, peaks appeared in 1427, 1350, 1316, 634 cm^{-1} corresponding to CH_2 bending, aliphatic CH bending, C–N stretch, aromatic CH bending, respectively. From the spectra of individual drugs and excipients, characteristic peaks of the drug were also seen in the FTIR spectrum of the physical mixture of CS, SL and cholesterol with no distinct change. This confirmed that there was no chemical interaction between the drug, lipid or cholesterol. These results are in conformity with previous reports [33]

Figure 1: FTIR spectra of (a) CS, (b) Cholesterol, (c) Phospholipid, (d) OCS-NSLs

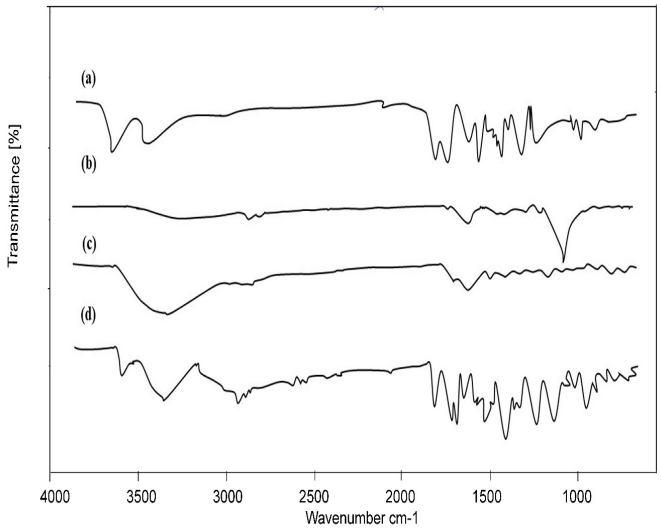

BBD Design for Optimization of Nano sized Liposomes

The CS-loaded NSL has been prepared using the conventional thin-layer hydration method [34]. Using the results of the preliminary and pre-optimization studies, three levels of each independent variable (factors) were determined (Table 2). For three factors and three levels, the Box-Behnken model has been selected. On applying three factors and three levels Box–Behnken statistical design, 17 runs with five central points were obtained with Design Expert 11 (Version 11.0, Stat-Ease Inc.,). All of these batches were prepared and assessed for responses such as % entrapping efficiency

(R1), particle size (R2), and *in vitro* drug release (R3). These 3D-plots are known to study the interaction effects of the factors on the responses as well as being useful in studying the effects of two factors on the response at one time which is shown in Figure 2. The actual and expected values as linear correlation graphs and the corresponding residual graphs for different responses were shown in the Figure 3.

All the results were placed in Box–Behnken design of Design Expert software to obtain the predicted values and final conclusion. All the responses of these runs fitted to first order, second order and quadratic models and the best fit model were quadratic ($p<.0001$) with insignificant lack of fit ($p>0.05$).

Table 2: Observed responses in Box–Behnken design for development and optimization

Factor 1	Factor 2	Factor 3	Response 1	Response 2	Response 3
Drug to Lipid ratio	Cholesterol	Sonication time	Entrapment Efficiency	Particle size	*In vitro* release
	mg	min	%	nm	%
0	-1	-1	80.57±1.23	229.65±10.32	88.25±0.54
0	1	1	88.53±1.98	220.43±11.32	70.54±0.35
0	0	0	82.32±1.87	240.12±17.54	82.54±1.23
-1	1	0	78.54±0.93	195.87±12.78	65.64±1.45
0	0	0	81.98±0.54	245.98±13.98	80.25±1.28
0	-1	1	79.76±1.98	230.54±12.09	89.52±1.56
1	0	1	92.76±2.08	264.32±11.97	82.83±0.34
1	1	0	96.74±1.76	275.98±10.34	71.45±1.24
0	0	0	83.87±0.65	242.87±11.76	80.54±0.67
1	0	-1	93.54±1.23	260.53±10.87	86.56±0.93
0	0	0	80.21±1.76	240.17±11.65	80.56±1.35
-1	0	1	76.54±1.98	192.65±16.98	79.56±1.27
-1	-1	0	74.21±1.45	200.98±19.87	85.25±0.23
-1	0	-1	75.98±1.76	210.96±12.76	72.92±0.76
1	-1	0	89.43±1.09	270.42±15.87	96.65±1.23
0	1	-1	87.62±0.25	235.42±12.82	62.86±1.45
0	0	0	81.24±2.43	238.87±12.63	81.26±1.78

Average ± SD for n =3

Figure 2: 3D-Response surface plots presenting the effect of three selected factors on (A) % EE of CS (B) Particle size (C) *In vitro* Drug release

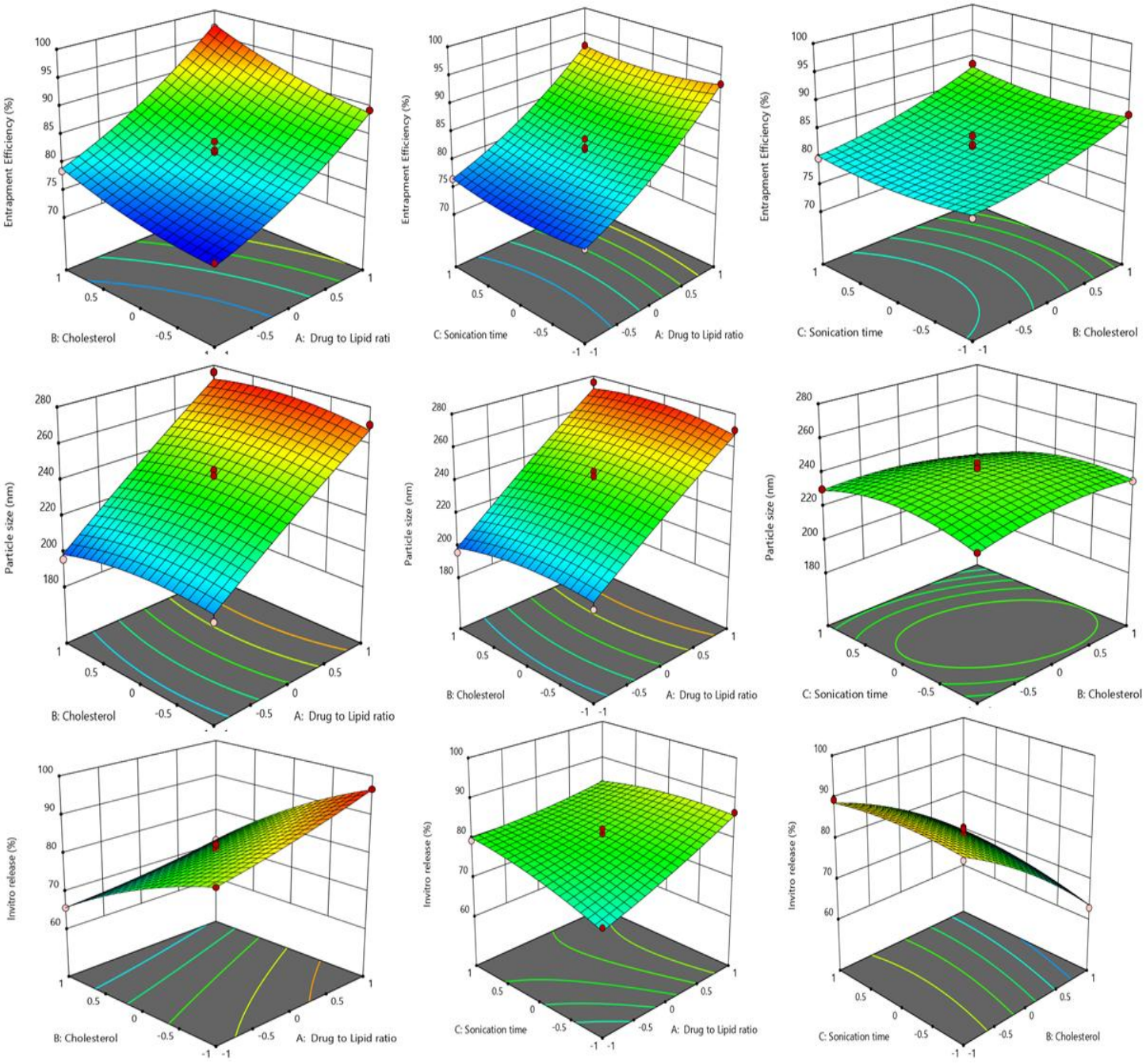

Response 1 (Y1): effect of independent variables on % EE of CS

The model F value of 55.85 suggested the model to be significant (< 0.0001). The "lack of fit" (F-value of 0.40) meant that it was nonsignificant (p=0.7604). The P values below 0.0500 indicate that the model terms are important. In this case X1, X2, X1X2, X2 X3, X_1^2, X_2^2 and X_3^2 in Equation (1) were significant model terms. Positive coefficients of factor X1, X2, X1X2, X2 X3, X_1^2, X_2^2, and X_3^2 exhibited the synergistic effect on % EE while negative coefficients of X2 and X1 X3 indicated the antagonistic effect on % EE.

% EE (Y1) = +81.92 + 8.40 X1 + 3.43 X2 - 0.0150 X3 + 0.7450 X1 X2- 0.3350 X1 X3 + 0.4300 X2 X3+1.70X_1^2 +1.11X_2^2 +1.09X_3^2 ---- (1)

The Predicted R^2 of 0.9327 was in reasonable agreement with the adjusted R^2 of 0.9686, indicating the adequacy of the model to predict the response of % EE. The "Adeq Precision" of 26.395 indicated an adequate signal. Therefore, this model was used to navigate the design space.

It was found that the average % EE of all 17 experimental trials was 83.75%, such that this value is between the minimum and maximum values 74.21% to 96.74%. The 3D-Response graph (Figure 2a) showed greater %EE of CS with increased drug to lipid content. Furthermore, cholesterol and sonication time also play an important role in the %EE, as the drug is trapped in the lipid phase.

On the base of the above polynomial equation, it was resolved that as the total lipid to drug concentration increases, the % EE of optimized formulation and this leads to more space for the accommodation of drug particle, likewise addition of lipid content as well reduces the escaping of drug into the external phase [35]. This could be due to denser vesicle lipid bilayers and an increased load of lipophilic CS in the lipid layer. Sonication time has an insignificant impact on EE. Cholesterol was added in the preparation because it helps the establishment of less leaky and rigid bilayers as it gets intercalated layers of lipid. It is clear from Table 2 that when cholesterol was used at a concentration of 15-25mg, the trapping increased significantly which is found similar as reported by El-Laithy et al. [36].

Response 2 (Y2): effect of independent variables on Particle size

The model F value of 56.69 suggested the model to be significant (< 0.0001). The "lack of fit" (F-value of 4.23) meant that it was non significant (p=0.0986). The P values below 0.0500 indicate that the model terms are important. In this case X1, X3, X1X2 and X1X3 in Equation (2) were significant model terms. Positive coefficients of factor X1, X2, X1X2 and X1X3, exhibited the synergistic effect of particle size while negative coefficients of X2, X2X3, X_1^2, X_2^2, and X_3^2 indicated the antagonistic effect on Particle size.

Particle Size (Y2) = +241.60 + 33.85X1-0.4862 X2+ 3.58X3 + 2.67X1 X2 + 5.53 X1 X3-3.97 X2 X3---1.34 X_1^2-4.45X_2^2 -8.14X_3^2---(2)

The Predicted R^2 of 0.8303 was in reasonable agreement with the adjusted R^2 of 0.9691, indicating the adequacy of the model to predict the response of % EE. The "Adeq Precision" of 26.395 indicated an adequate signal. Therefore, this model was used to navigate the design space.

It was found that the average particle size of all 17 experimental trials was 235.0447nm, such that this value is between the minimum and maximum size values 192.65nm to 275.98nm.

The 3D-Response graph (Figure 2b) showed greater particle size of CS with increased drug to lipid content. Furthermore, cholesterol also plays an important role in the particle size, and sonication time has negligible effect. The size of the vesicle was also increased from 192.65 12.62 nm to 270.42 9.65 nm, when the quantity of lecithin in the preparation was increased. Likewise, when the amount of cholesterol has increased from 5 to 15 mg, the size of the vesicle increases from 200.98 ± 12.67 nm to 264.32 ± 10.30 nm [37]. Increased cholesterol levels (15-25mg) also contributed to an increase in hydrophobicity, followed by a slight reduction in the size of the vesicle [38, 39]. Also, the incorporation of lipophilic drugs into the hydrophobic domain of vesicle causes the bilayer molecules to move apart from each other, leading to an increase in vesicle size [40].

Response 3 (Y3): effect of independent variables on *in vitro* drug release

The amount of CS (%) released after 24 h at different levels of the three factors (X1, X2, and X3) was subjected to multiple regressions to get the following second-order polynomial equation in Equation (3) The model F value of 119.39 suggests that the model was significant (p < 0.0001). The "lack of fit" (F-value of 1.80) meant that it was non significant (p= 0.2865). P-values less than 0.0500 indicate model terms are important. In this case X1, X2, X3, X2X3, and X_1^2 were significant model terms. Positive coefficients of factor X1, X2, X3, X2X3 and X_1^2 exhibited the synergistic effect on % *in vitro* release while negative coefficients of X1X2, X1X3, X_2^2, and X_3^2 indicated the antagonistic effect on % *in vitro* release.

% *In vitro* Release (Y3) =+81.03 + 4.27X1 +11.15X2 +1.48X3 – 1.40X1X2 -2.59X1X3 +1.60 X2X3+0.6962 $X1^2$-1.98$X2^2$-1.26$X3^2$----(3)

The Predicted R^2 of 0.9362 was in reasonable agreement with the adjusted R^2 of 0.9852, indicating the adequacy of the model to predict the response of % *in vitro* release. The "Adeq Precision" of 40.250 indicated an adequate signal. Therefore, this model was used to navigate the design space.

The average % *in vitro* release of all the 17 experimental runs was found to be 79.83 ± 1.45%, hence these values lie between

the minimum and maximum value of the size 62.86 ± 1.24 % to 96.65 ± 0.98%. The %CS released after 24 h from the different liposomal formulae showed a wide variation ranged from 62.86 ± 1.24 % to 96.65 ± 0.98% (Table 2). The 3D-Response graph (Figure 2c) showed greater % *in vitro* release of CS with increased drug to lipid content. Furthermore, cholesterol also plays an important role in the % *in vitro* release, and sonication time has optimum effect.

The decrease in % CS released is found due to an increase in the cholesterol concentration. This high cholesterol concentration led to reduce the membrane permeability by lowering the membrane fluidity and thus hindering the entrapped CS to escape. Therefore, CS released from the liposome vesicles was reduced [41].

The optimization was done based on the principle of achieving the desirable values of % EE, particle size and *In vitro* drug release by applying numerical point prediction method. The formulation composition with drug to lipid ratio (1:4), Cholesterol (25mg), and Sonication time (10 min) has been set up to comply with the demands. The optimized Carmustine nanosized liposomes (OCS-NSLs) presented the practical values of %EE of CS is 94.27 ± 0.25%, Particle size of 235.65 ± 12.87 and *in vitro* drug release of CS 97.089 ± 1.76%. These practical values of %EE of CS, Particle size and *in vitro* drug release yielded by the OCS-NSLs formulation were found in conformity with the predicted value of %EE of CS is 91.27 ± 0.25%, Particle size of 242.35 ± 10.87 and *in vitro* drug release of CS 96.099 ± 1.66%.

Figure3: Actual and predicted values as linear correlation plots (A, C, E, and G) and the corresponding residual plots (B, D, F, H) for various responses

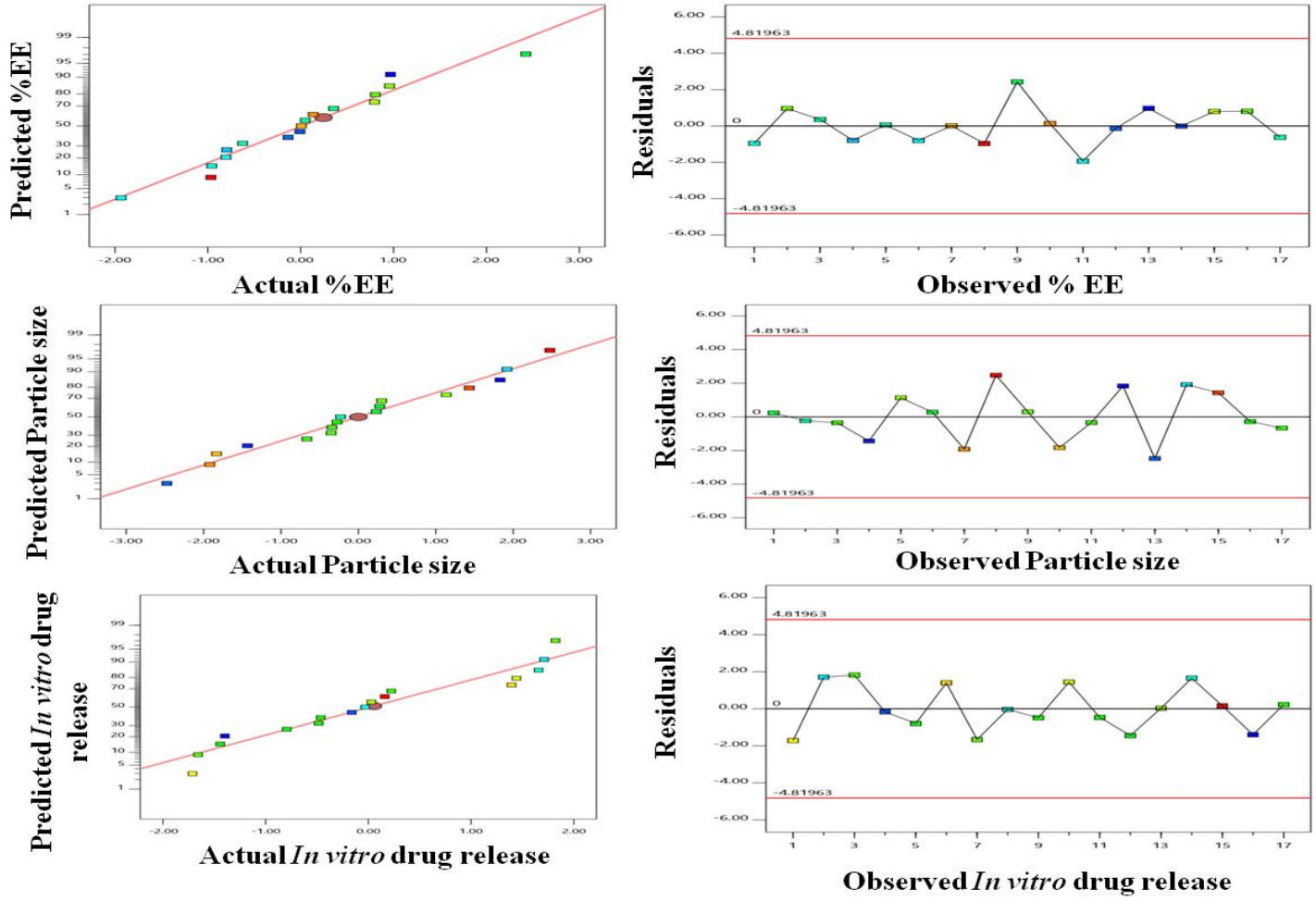

Characterization of optimized NSL

Particle size, PDI and Zeta Potential

The mean particle size for OCS-NSL was 235.65 ±12.87 nm, which proved appropriate for nasal brain targeting. PDI value was 0.124, indicating the uniformity of the particle size of the developed NSLs [19]. The particle size for OCS-NSLs is illustrated in Figure 4. The zeta potential of optimized formula was −51.4 mV (Figure 5). The mean particle size proved appropriate for nasal brain targeting. The PDI is primarily the ratio of the standard deviation to the average particle size. Owing to tight junctions present in the nasal epithelial cells, which open and shut down in accordance to activation of signaling mechanisms, however size plays a significant function in relation to absorption through intranasal route [37]. A PDI value equal to or less than 0.3 indicates uniform particle size. The Zeta potential is the measure of the electric charge that is on the surface of the particles. The zeta potential is the electrostatic charge of the particle surface which acts as a repulsive energy barrier controlling the

stability of dispersion and opposing the proximity of the particles and aggregation. This high potential for zeta (±40 to ±60 mV) indicates that the lipid formulation [42] is stable.

Figure 4: Particle size distribution of OCS-NSLs

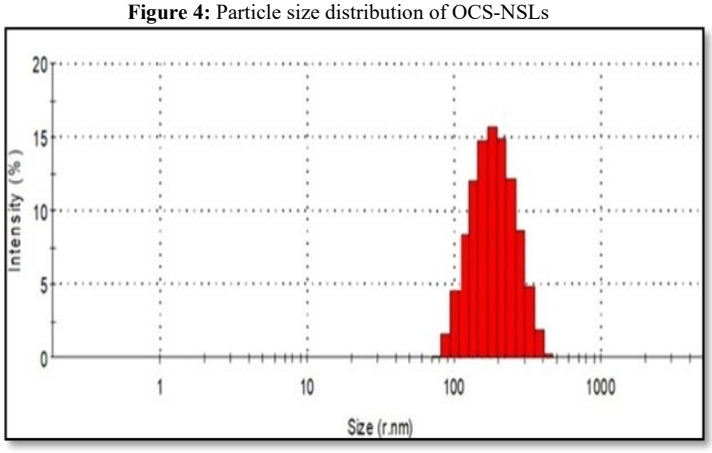

Figure 5: Zeta Potential of OCS-NSLs

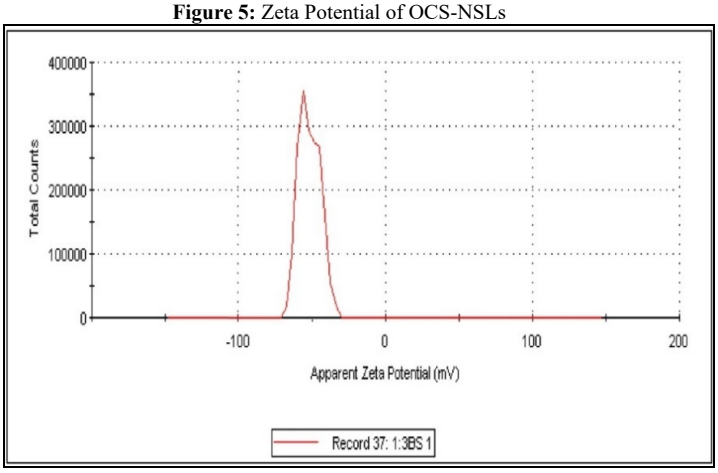

Vesicular shape and surface morphology

Transmission electron microscopy (TEM) images of OCS-NSLs as shown in Figure 6 revealed that particle sizes were 240 nm. Transmission electron microscopy (TEM) images from OCS-NSLs showed spherical form and uniform distribution of liposomes. It showed a mono dispersed distribution without any aggregation [43].

Figure 6: TEM image of OCS-NSLs

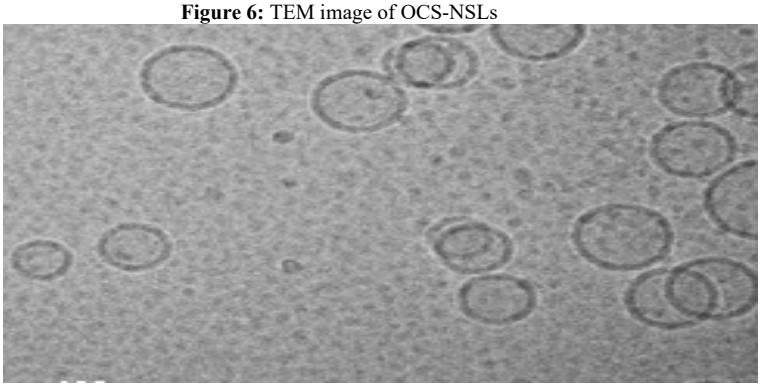

Scanning Electron Microscopy

The size of OCS-NSLs using SEM (Figure 7) was found to be 250 nm, which is well correlated with the particle size obtained with particle size analyzer. The external morphological structure of the OCS-NSLs was investigated using SEM, which revealed the spherical size of the NSL, and neither drug crystal nor particle aggregation was observed. The result of particle size was found to be in good agreement with the result established by SEM study [44].

Figure 7: SEM image of OCS-NSLs

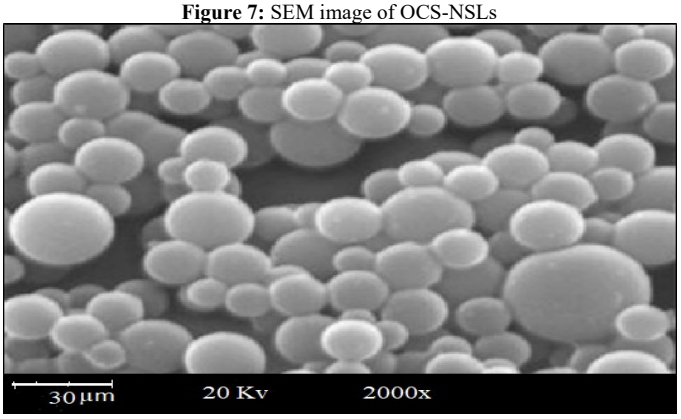

***In vitro* drug release study**

The comparative *in vitro* release of CS from the experimental formulation (NSLs) and free-drug solution was done by dialysis method and the result was expressed as cumulative drug release percentage against time in hour (h). More than 95% of CS released within 6 h from free drug solution. The release of CS from free-drug solution was faster than NSL-OCS. The maximum release of CS from the NSL-OCS is 95.13 ± 1.230% up to 24 hrs (Figure 8). The OCS-NSLs showed the initial burst release of 30.94 ± 6.29%. Thereafter, OCS-NSLs showed sustained drug release with maximum drug release of 95.13 ± 1.230% in 24 h. OCS-NSLs showed the biphasic release from the prepared NSL, initially the drug release rapidly from the lipid surface, tracing the slow freeing of the drug owing to degradation of lipid core. The initial burst release may be ascribed to the presence of free drug in the external phase and adsorbed drug onto the surface of particles, while the slow release may be owed to the encapsulated drug within the lipid matrix [19,45].

Figure8: *In vitro* drug release of OCS-NSLs. Data show mean ± SD (n =3)

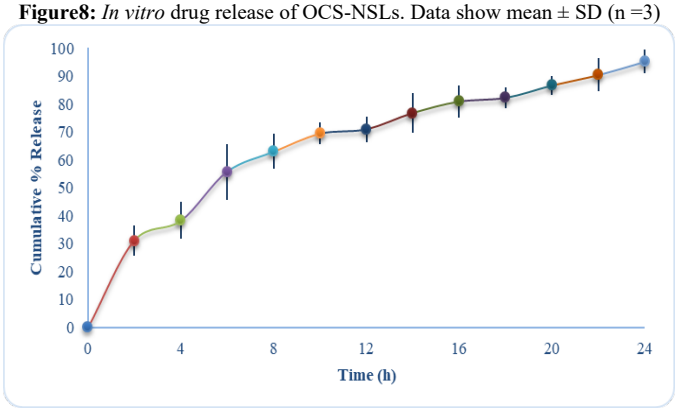

Estimation of drug release kinetics

Widely used mathematical models such as zero order, first order, Higuchi and Korsemeyer-Peppas were applied to determine release kinetics from an optimized formulation (Table 3). Higuchi's equation was the best fit model as $r^2 > 0.99$ suggesting the diffusion-controlled release between 5–24 h as shown in Figure 8. This result

supports the fact that the vesicle lipid bilayer acts as a factor limiting the slow and controlled release rate of the drug when administered. Similar results were observed by Afzal Hussain [35] who developed elastic vesicular liposomes loaded with Rifampicin. Therefore, prolonged drug release is achieved, where the lipid bilayer acts as a rate limiting membrane for CS diffusion across its membrane [46].

Table 3: Release kinetic models for OCS-NSLs formulation

Optimized	Zero order (r^2)	Higuchi model	Korsmeyer–Peppas		First order(R^2)
			(r^2)	n	
ONSLs	0.857	0.996	0.945	0.570	0.927

CONCLUSIONS

Liposomal carrier has been optimized for intranasal administration of CS. OCS-NSLs has been developed with the help of the BBD design, which presents an optimized preparation of the best particle size and trapping efficiency. A reasonable drug encapsulation was reported to OCS-NSLs along with a sustained drug release property in a 24 h study period. Thus, OCS-NSLs serve as potential drug delivery vehicles in treating glioblastoma effectively *invitro*.

ACKNOWLEDGMENT

The author is thankful to JNTUA-OTPRI, Ananthapuramu for providing the laboratory facilities, chemicals to carry out the research work.

DECLARATION

The authors declared that they have no conflicts of interest.

REFERENCES

1. Matthias Preusser, Sandrine de Ribaupierre, Adelheid Wöhrer, 2011. Current concepts and management of glioblastoma, Ann Neurol. 70: 9–21.
2. Johnson KJC, Cullen J, Barnholtz Sloan JS, 2014. Childhood brain tumor epidemiology: a brain tumor epidemiology consortium review, Cancer Epidemiol Biomarkers Prev. 23: 2716-36.
3. Quinn T Ostrom, Luc Bauchet, Faith G Davis, 2014. The epidemiology of glioma in adults: a state of the science review, Neurol Oncol. 16: 896-913.
4. Wiemels J, Wrensch M, Claus EB, 2010. Epidemiology and etiology of meningioma, J Neurooncol 99: 307-14. .
5. Ambikanandan Misra, Ganesh S, AliasgarShahiwala, 2003. Drug delivery to the central nervous system: a review, J Pharm Pharm Sci. 6: 252–273.
6. Lucia Gastaldi, Luigi Battaglia, Elena Peira, 2014. Solid lipid nanoparticles as vehicles of drugs to the brain: current state of the art, Eur J Pharm Biopharm. 87: 433–444.
7. Illum L, 2002. Nasal drug delivery: new developments and strategies, Drug Discov Today.7: 1184–1189.
8. Krishnamoorthy R, Mitra AK, 1998. Prodrugs for nasal drug delivery, Adv Drug Deliv Rev. 29: 135–146.
9. Shagufta Khan, Kundan Patil, Nishan Bobade, 2010. Formulation of intranasal mucoadhesive temperature-mediated in situ gel containing ropinirole and evaluation of brain targeting efficiency in rats, J Drug Target. 18: 223–234.
10. Weiss RB, Issell BF, 1982. The nitrosoureas: Carmustine (BCNU) and Lomustine (CCNU), Cancer Treat Rev. 9: 313–330.
11. Alam MI, Beg S, Samad A, 2010. Strategy for effective brain drug delivery, Eur J Pharm Sci. 40(5): 385-403.
12. Khan AR, Liu M, Khan MW, 2017. Progress in brain targeting drug delivery system by nasal route, J Control, Release 268: 364–389.
13. Bourganis V, Kammona O, Alexopoulos A, 2018. Recent advances in carrier mediated nose-to-brain delivery of pharmaceutics, Eur, J Pharm, Biopharm. 128, 337–362.
14. Driscoll BR, Kalra S, Gattamaneni HR, 1995. Late Carmustine lung fibrosis. Age at treatment may influence severity and survival, Chest. 107: 1355–1357.
15. Lin SH, Kleinberg LR, 2008. Carmustine wafers: localized delivery of chemotherapeutic agents in CNS malignancies, Expert Rev Anticancer Ther. 8: 343–359.
16. Muntimadugu E, Dhommati R, Jain A, 2016. Intranasal delivery of nanoparticle encapsulated tarenflurbil: A potential brain targeting strategy for Alzheimer's disease, Eur. J Pharm, Sci. 92, 224–234.
17. Prokop A, Davidson JM, 2008. Nanovehicular intracellular delivery systems, Journal of Pharmaceutical Sciences. 97(9):3518-3590.
18. Gloria Invernici, Silvia Cristini, Giulio Alessandri, 2011. Nanotechnology advances in brain tumors: the state of the art, Recent Pat Anticancer Drug Discov. 6: 58–69.
19. Mohd Yasir, Udai Vir Singh Sara, Iti Chauhan, 2017. Solid lipid nanoparticles for nose to brain delivery of donepezil: Formulation, optimization by Box–Behnken design, *in vitro* and *in vivo* evaluation, Artificial cells, nanomedicine, and biotechnology. 46(8): 1-14.
20. Tapan Kumar Shaw, Dipika Mandal, Goutam Dey, 2017. Successful delivery of docetaxel to rat brain using experimentally developed nanoliposome: a treatment strategy for brain tumor, Drug Deliv. 24: 346–57.
21. Ahad A, Raish M, Al-Mohizea AM, 2014. Enhanced anti-inflammatory activity of carbopol loaded meloxicam nanoethosomes gel, Int J Biol Macromol. 67: 99–104.
22. Mohd Qumbara, Ameeduzzafar, Syed Sarim Imam, 2017. Formulation and optimization of lacidipine loaded niosomal gel for transdermal delivery: *In-vitro* characterization and *in-vivo* activity, Biomed. Pharmacother. 93: 255–266.
23. Natarajan Jawahar, Prashant Kumar Hingarh, Radhakrishnan Arun, 2018. Enhanced oral bioavailability of an antipsychotic drug through nanostructured lipid carriers, Int J Biol Macromol. 110: 269-275.
24. Hardevinder Pal Singh, Puneet Utreja, Ashok Kumar Tiwary, 2009. Elastic liposomal formulation for sustained delivery of colchicine: *in vitro* characterization and *in vivo* evaluation of anti-gout activity, AAPS J 11(1): 54–64.
25. Shan Lu, Pan-pan Yu, Jian-Hua He, 2016. Enhanced dissolution and oral bioavailability of Lurasidone hydrochloride nanosuspensions prepared by anti-solvent precipitation-ultrasonication method, RSC Adv. 6: 49052-59.
26. Jawahar Natarajan, Mahendran Baskaran, Lireni C Humtsoe, 2017. Enhanced brain targeting efficacy of olanzapine through solid lipid nanoparticles, Artif Cells NanomedBiotechnol. 45: 364-371.
27. Khan R, Irchhaiya R, 2020. *In vitro in vivo* evaluation of niosomal formulation of famotidine, Int J Pharm Pharm Sci. 12: 15-22.
28. Sailaja PB, Jeevana JB, 2020. Development and *in vitro* evaluation of 5-fluorouracil nanoparticles by salting out technique, Asian J Pharm Clin Res. 13: 166-71.

29. Mandpe L, Pokharkar V, 2015. Quality by design approach to understand the process of optimization of iloperidone nanostructured lipid carriers for oral bioavailability enhacement, Pharm Dev Technol. 20: 320-329.
30. Higuchi T, 1963. Mechanism of sustained- action medication. Theoretical analysis of rate of release of solid drugs dispersed in solid matrices, J Pharm, Sci. 52: 1145–1149.
31. Korsmeyer RW, Gurny R, Doelker E, 1983. Mechanisms of solute release from porous hydrophilic polymers, Int J Pharm. 15: 25– 35.
32. Posina Anitha, Sundarapandiyan Ramkanth, Mohamed TS Saleem, et al, 2011. Preparation, *in-vitro* and *in-vivo* characterization of Transdermal patch containing Glibenclamide and Atenolol: a combinational approach. Pak J Pharm Sci. 24: 155-63.
33. Shufeng Yi, Fan Yang, Cunle Jie, et al, 2019. A novel strategy to the formulation of carmustine and bioactive nanoparticles co-loaded PLGA biocompositespheres for targeting drug delivery to glioma treatment and nursing care. Artif Cells NanomedBiotechnol. 47(1): 3438-3447.
34. Francesca Maestrelli, Maria Luisa Gonzalez-Rodrıguez, Antonio Maria Rabasco, et al, 2005. Preparation and characterization of liposomes encapsulating ketoprofen–cyclodextrin complexes for transdermal drug delivery. Int J Pharm. 298: 55–67.
35. Afzal Hussain, Mohammad A. Altamimia, Sultan Alshehria, Syed Sarim Imam,et al, 2020. Vesicular elastic liposomes for transdermal delivery of rifampicin: *In-vitro*, *in-vivo* and in silico GastroPlus™ prediction studies. European Journal of Pharmaceutical Sciences. 151: 105411.
36. El-Laithy HM, Shoukry O, Mahran LG, 2011. Novel sugar esters proniosomes for transdermal delivery of vinpocetine: preclinical and clinical studies, Eur. J. Pharm. Biopharm. 77: 43–45.
37. Javed Ali, Imrana Jazuli, Annu, Bushra Nabi, et al, 2019. Optimization of Nanostructured Lipid Carriers of Lurasidone Hydrochloride Using Box-Behnken Design for Brain Targeting: *In Vitro* and *In Vivo* Studies. Journal of Pharmaceutical Sciences. 108: 3082-3090.
38. Akhtar M, Imam SS, Ahmad MA, et al, 2014. Neuroprotective study of Nigella sativa-loaded oral provesicular lipid formulation: *in-vitro* and *ex-vivo* study, Drug Deliv. 21: 487–494.
39. Zidan AS, Mokhtar M, 2011. Multivariate optimization of formulation variables influencing flurbiprofen proniosomes characteristics, J Pharm Sci. 100: 2212–2221.
40. Syed Sarim Imam, Mohammed Aqil, Mohammed Akhtar, 2015. Formulation by design-based proniosome for accentuated transdermal delivery of risperidone: *in vitro* characterization and *in vivo* pharmacokinetic study, Drug Deliv. 22(8): 1059–1070.
41. Hathout RM, Mansour S, Mortada ND, 2007. Liposomes as an ocular delivery system for acetazolamide: *in-vitro* and *in-vivo* studies, AAPS PharmSciTech. 8: 1–8.
42. Soha Ismail, Abeer Khatta, 2018. Optimization of proniosomal Itraconazole formulation using Box Behken design to enhance oral bioavailability, J Drug Deliv Sci and Tech. 45: 142–150.
43. Costantino HR, Illum L, Brandt G, 2007. Intranasal delivery: physiochemical and therapeutic aspects, Int J Pharm. 337: 1-24.
44. Wen MM, Farid RM, Kaseem AA, 2014. Nano-proniosomes enhancing the transdermal delivery of mefenamic acid, J Liposome Res. 24: 280–289.
45. Ashwini S Joshi, Hitesh S Patel, 2012. Solid lipid nanoparticlesof ondansetron HCl for intranasal delivery: development, optimization and evaluation, J Mater Sci Mater Med. 23: 2163–2175.
46. Cevc G, 2003. Transdermal drug delivery of insulin with ultradeformable carriers, Clin Pharmacokinet. 42: 461–474.

How to cite this article

M Alagusundaram, K B ChandraSekhar, G Nethra Vani, 2022. Nano-sized Liposomes for nose to brain delivery of Carmustine Formulation, Optimization by Box Behnken design. J. Med. P'ceutical Allied Sci. V 11 - I 2, Pages - 4518 – 4526. doi: 10.55522/jmpas.V11I2.2159.